EDGE ILLUMINATION X-RAY PHASE CONTRAST IMAGING AND ULTRASONIC ATTENUATION FOR POROSITY QUANTIFICATION IN COMPOSITE STRUCTURES

Dana Shoukroun
Department of Medical Physics and Biomedical Engineering, UCL, WC1E 6BT, UK

Sandro Olivo
Department of Medical Physics and Biomedical Engineering, UCL, WC1E 6BT, UK

Paul Fromme
Department of Mechanical Engineering, UCL, WC1E 6BT, UK

ABSTRACT

Carbon fiber reinforced composites are widely used in the aerospace industry, due to their low weight and high strength. Porosity often occurs during the manufacturing of composite structures, which can compromise the structural integrity of the part and affect its mechanical properties. In the aerospace industry a typical requirement for structural components is for the porosity content to be kept below 2%. Non-destructive evaluation (NDE) techniques are used to estimate the porosity content in composite components, the most common being ultrasonic attenuation and X-ray computed tomography (CT).

Planar Edge Illumination X-ray Phase Contrast Imaging (EI XPCI) was used to quantify the porosity content in woven carbon fiber reinforced composite plates with porosity ranging between 0.7% and 10.7%. A new metric was introduced, the standard deviation of the differential phase (STDVDP) signal, which represents the variation of inhomogeneity in the plates for features of a scale equal to or above the system resolution (here 12µm). The SDTVDP was found to have a very high correlation with porosity content estimated from matrix digestion and ultrasonic attenuation, hence providing a promising new methodology to quantify porosity in composite plates.

Keywords: Radiography, XPCi, ultrasound, porosity, CFRP.

1. INTRODUCTION

Porosity in carbon fiber reinforced composites often occurs during manufacturing. For the aerospace industry, a typical target is to ensure that porosity is kept below 2% [1]. Porosity is defined as a series of sub-millimeter micro-voids that can affect the mechanical integrity of a structure [2]. Different non-destructive evaluation (NDE) techniques are employed to detect and quantify porosity in composite plates, the most common methods being ultrasonic attenuation [3] and X-ray CT imaging [4]. However, both techniques have limitations, with ultrasonic attenuation imaging limited by a relatively low resolution, whereas X-ray CT imaging has relatively long acquisition times. There also exist different destructive evaluation techniques, such as micrography [5] and matrix digestion [6], that can provide a better characterization of porosity in composite plates, however are destructive and thus cannot be used for monitoring purposes.

Edge Illumination X-ray Phase Contrast Imaging (EI XPCi) is a novel technique that relies on the phase effects that take place when X-rays pass through a material. In conventional radiography, the contrast produced relies on the attenuation coefficient and on the thickness of the feature through which the X-rays pass, which can lead to weak contrast in cases where two adjacent features have similar attenuation coefficients, or alternatively, where the thickness of the feature of interest is too thin to cause a significant change in the attenuation of the X-rays. X-ray phase contrast imaging allows for a better contrast as it relies on the real part of the refractive index, meaning that the introduction of an object into the beam causes a distortion to the X-ray and changes its direction of propagation [7]. There are different X-ray phase contrast imaging methods [8, 9]. EI XPCi uses a set of coded apertures to convert the phase effects into a variation of detected intensity. It is known as a differential phase imaging method, meaning it measures the refraction angle that accompanies the X-ray distortion, which is the first derivative of the phase change. Using acquisition of at least three images, EI XPCi allows for the simultaneous retrieval of the standard attenuation, differential phase, and dark field signals, with the latter signal due to features in the sub-pixel scale [10].

Various XPCi methods were used for nondestructive evaluations of damage and porosity in composites [9, 11, 12], and EI XPCi was shown to be able to detect different types of damage in a severely damaged composite plate [13]. The complementarity offered by the multiple signals allowed the detection of different defects as they showed up in the different signals, as well as offering an indication of their length scales and their full extent using the dark field signal. These observations were confirmed by comparison to both high-resolution conventional X-ray CT imaging and ultrasonic immersion C-scan imaging [14].

In this contribution, the quantification of porosity in woven composites plates with varying degrees of porosity is demonstrated, by introducing the standard deviation of the differential phase as a new metric in EI XPCi [15], and comparing it to ultrasonic attenuation and the destructive matrix digestion analysis.

2. MATERIALS AND METHODS

A set of nine 100*50mm^2 carbon-reinforced woven composite specimens were used in this investigation, extracted from larger composite panels. All nine panels were manufactured with a layup of 10 pre-preg M21 epoxy carbon

woven fabric plies, using the standard autoclave cure recommended by Hexcel for M21 plies. The cure parameters were such that the panels were pressurized to 7bar, with 100% vacuum for the duration of the cure, and heated at 2˚C/min, dwelled at 180˚C for 120min, and subsequently cooled at 5˚C/min. When the temperature reached 60˚C, panels were depressurized. Variations of the cure led to plates with different porosity, varying from 0.7% to 10.7%. Small parts were extracted from the panels adjacent to the extracted plate for the quantification of porosity using matrix digestion, using nominal densities of 1280kg/m^3 for the matrix and 1780kg/m^3 for the fibers [6]. The specimens were split into 18 regions of interest (ROIs) of size 15*15mm^2 using reflective tape due to the small field of view of the X-ray system, as shown in Fig. 1, and were scanned one ROI at a time, resulting in 75% of the plate being scanned around the edges.

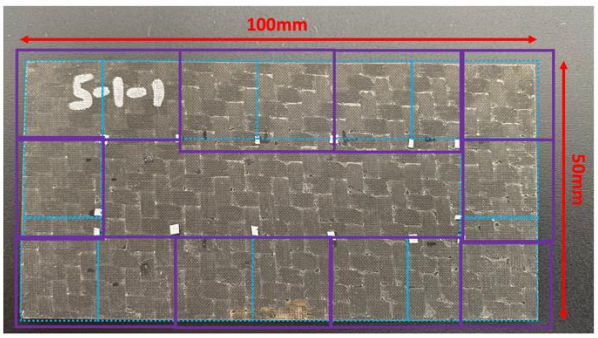

FIGURE 1: POROSITY PLATE SPECIMEN WITH REFLECTIVE TAPE AND 18 REGIONS OF INTEREST (ROI) MARKED.

The nine plate specimens were scanned using ultrasonic immersion through transmission C-scan imaging. A pair of 5MHz focused transducers, immersed in water, were placed on either side of the sample. The emitting transducer (Olympus U8420169) had a 0.5in (13mm) nominal diameter, 0.75in (19mm) focal length and 650µm focal spot diameter, with 300µm wavelength. The receiving transducer (Ultran XL50-5-P3) had a 0.5in (13mm) nominal diameter, 3in (76mm) focal length and 2.6mm focal spot diameter. The experimental setup is shown in Fig. 2, where a pulse is emitted by the transducer, connected to a pulser/receiver, and propagates through the sample onto the receiving transducer, also connected to the pulser/receiver. The received signal is recorded by an oscilloscope (LeCroy 9304) and saved as the full A-scan for each measurement point. The plates were scanned using a 500µm step size, resulting in a 221 by 121 step scan to contain the whole specimen. The A-scans were then used to calculate the ultrasonic signal attenuation, by comparing the maximum amplitude of the A-scans through the sample to the amplitude of the signal transmitted only through water, using equation 1:

$$\Delta I(dB) = 20 * \log \frac{V_{water}}{V_{sample}} \qquad (1)$$

where ΔI is the ultrasonic signal attenuation in decibels (dB), V_{water} is the maximum signal amplitude in water in Volts (V) and V_{sample} is the maximum signal amplitude through the sample, also in Volts (V).

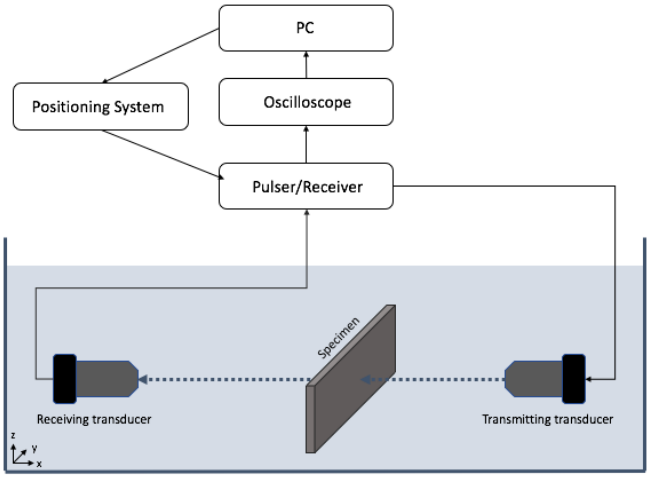

FIGURE 2: EXPERIMENTAL SETUP USED FOR THE SINGLE THROUGH TRANSMISSION ULTRASONIC C-SCAN IMAGING.

The EI XPCi setup used to scan the nine specimens is shown in Fig. 3. Two coded aperture masks were used in the system: a first mask, the sample mask, was placed upstream of the sample and splits the X-ray beam into beamlets. A second mask, called the detector mask, was placed adjacent to the detector, and made the area between neighboring pixels insensitive to incoming X-rays. The sample mask had an aperture of 12µm and a period of 78µm; the detector mask had an aperture of 20µm and a period of 98µm. The masks were made of graphite with a gold substrate and produced by MicroWorks. The masks used in this setup were "skipped" masks, meaning every other pixel of the detector was made insensitive to incoming X-rays. This was done in order to avoid crosstalk between neighboring pixels. The source used was a Rigaku MicroMax 007 HF molybdenum, rotating anode source operating at 40kVp and 20mA, with a 70µm focal spot. The detector used was an indirect flat panel CMOS detector with 50*50µm^2 pixels. The source to detector distance was 0.85m, and the sample mask was place 0.7m away from the source, with the sample placed 0.75m away from the source [16]. The system was only sensitive to phase effects along the x-direction, and the system magnification was 1.25. The image acquisition process included the acquisition of the illumination curve (IC), which is a bell-shaped curve that corresponds to the variation in detected intensity for different positions of the sample mask relative to the detector mask. This was done by acquiring 19 flat fields at 19 relative sample mask positions, with 9 flat fields symmetrically taken on either side of the curve and one where the sample mask is aligned with the detector mask, corresponding to the top of the curve.

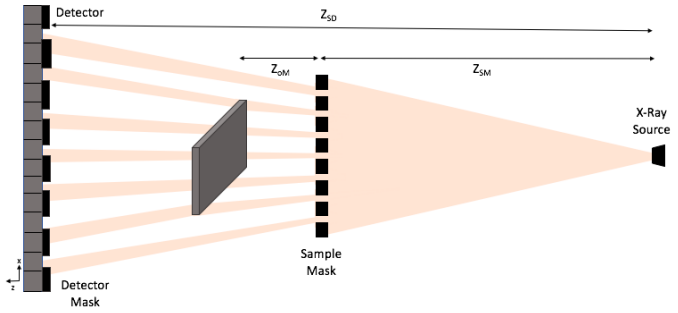

FIGURE 3: EXPERIMENTAL SETUP USED FOR THE EDGE ILLUMINATION X-RAY PHASE CONTRAST IMAGING.

The sample was then introduced, and another 19 images were taken with the same relative sample mask positions as the IC. All images were acquired with 6s exposure time. Additionally, the samples were dithered 16 times, i.e., repositioned at different sub-pixel locations, in order to increase the resolution along the x-direction to the aperture size of the sample mask, i.e., 12µm. In the y-direction, the resolution was determined by the detector performance, i.e., 100µm. The phase retrieval used for these samples is explained in [17], where a Gaussian is fitted to the IC and the sample images and the attenuation, differential phase, and dark field signals are retrieved by comparing the Gaussian parameters with and without the sample in the beam on a pixel-by-pixel basis. The attenuation signal corresponds to the amplitude of the Gaussian, the differential phase corresponds to the shift in the Gaussian central position, and the dark field signal corresponds to the broadening of the Gaussian curve.

A new metric is introduced here, the standard deviation of the differential phase (STDVDP). This metric, similar to the dark field signal, is capable of measuring variations in the distribution of the sample inhomogeneities, however for features of a scale equal to or above the system resolution (i.e., 12µm in the x-direction).

3. RESULTS AND DISCUSSION

C-scans of ultrasonic signal attenuation for the different specimens were created, with two representative plate results shown in Fig. 4, one with low porosity (0.9%) and a high porosity plate (5.9%). It can be observed that the high porosity plate shows high ultrasonic signal attenuation, with an average of 28.4±6.3dB. It can also be observed that the porosity distribution is not uniform, with the highest concentration of the porosity found in the bottom right corner, and the left side of the sample showing relatively low attenuation. The woven structure of the plate is also somewhat visible in the C-scan, with the porosity seemingly following the woven structure. The low porosity plate shows substantially lower and rather uniform signal attenuation, with an average of 9.3±1.2dB. The low porosity across the plate appears to be very uniform, with the yellow dots observed corresponding to the reflective tape used to delimit the different ROIs.

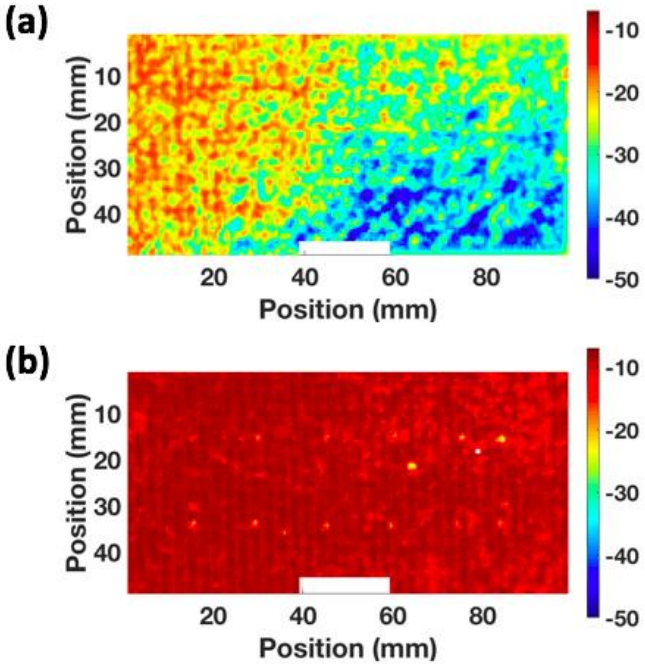

FIGURE 4: C-SCANS OF ULTRASONIC SIGNAL ATTENUATION FOR TWO PLATES (50MM*100MM) WITH POROSITY OF 5.9% (A) AND 0.9% (B); COLOR BAR INDICATES ULTRASONIC SIGNAL ATTENUATION.

The average ultrasonic signal attenuation was calculated for each ROI across all nine plates and compared to the three EI XPCi channels. As expected, almost no correlation was found between the ultrasonic signal attenuation and the X-ray attenuation signal, as the only variation observed through the attenuation signal corresponds to variation in the sample thickness, and X-ray attenuation has low sensitivity to the presence of porosity. No correlation was found between the ultrasonic signal attenuation and the differential phase either; this is expected as the positive and negative values of the differential phase signal due to different interfaces average to zero. The main channel that was expected to show a correlation for porosity measurement was the dark field signal, as it gives an indication of the variation in the distribution of inhomogeneities across the sample. However, here too, only limited correlation was found between the ultrasonic signal attenuation and the dark field signal. This is due to a number of reasons: First, the resolution of the EI XPCi system is equal to the sample mask aperture, i.e., 12µm, meaning that the dark field channel is sensitive to features below that resolution. However, the resolution of the ultrasonic scan is determined by the step size, focal spot, and wavelength, which were all significantly larger (>300µm). As a result, the ultrasonic beam is not sensitive to the features observed in the dark field channel, and cannot be easily compared. Moreover, upon inspection of the retrieved X-ray images, it was observed that the porosity features are visible in

the differential phase images, and not in the dark field signal, indicating that the size of the porosity features are of a size equal to or above the system resolution and as a result cannot be fully quantified using the dark field signal alone.

Since neither the differential phase nor the dark field channels was able to quantify the porosity on their own, the standard deviation of the differential phase (STDVDP) was introduced. STDVDP is considered as the equivalent of the dark field signal for features of a scale equal to or above the system resolution, showing the variation in the distribution of inhomogeneities across the plates, and as a result representing the degree of porosity. A comparison of the ultrasonic signal attenuation for the individual ROIs across all nine plates with the corresponding STDVDP is shown in Fig. 5.

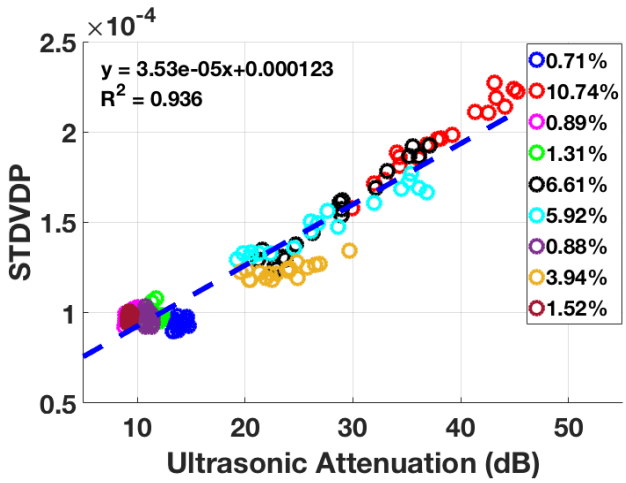

FIGURE 5: STANDARD DEVIATION OF THE DIFFERENTIAL PHASE SIGNAL (STDVDP) FOR EACH INDIVIDUAL ROI COMPARED WITH ULTRASONIC ATTENUATION FOR ALL NINE PLATES.

A very good correlation can be observed between the STDVDP and the ultrasonic signal attenuation of the ultrasonic signal for the individual ROIs for all nine plates, with an R^2 of 0.93. A very strong correlation can be especially observed for the highest porosity plates, with both measures correlating well for variation within and between specimens. One of the mid-porosity plates (3.4%) was observed to exhibit a slightly different correlation (different gradient) than the other high porosity plates. The lower porosity plates (below 2%) show less of a variation for the STDVDP, whereas the ultrasonic signal seems to indicate some variation between the different plates. In order to better compare the two signals, the average ultrasonic signal attenuation and STDVDP was calculated for each individual plate, and the two are plotted against each other in Fig. 6.

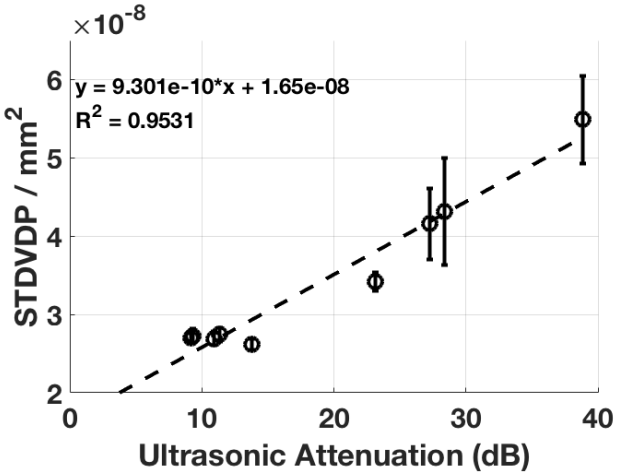

FIGURE 6: OVERALL STANDARD DEVIATION OF THE DIFFERENTIAL PHASE SIGNAL (STDVDP, AVERAGE AND STANDARD DEVIATION) COMPARED WITH AVERAGE ULTRASONIC SIGNAL ATTENUATION FOR ALL NINE PLATES.

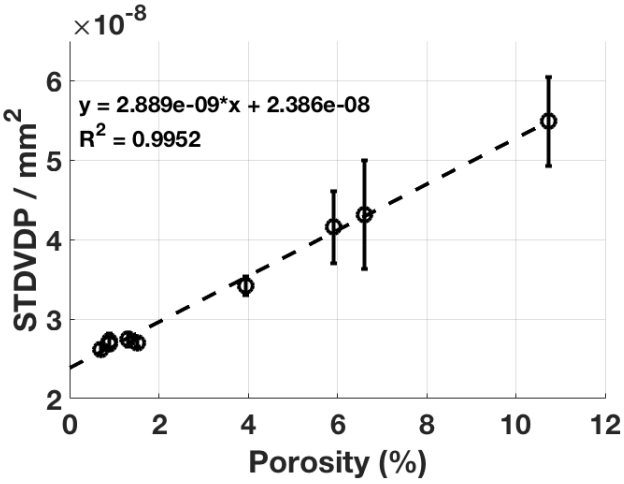

FIGURE 7: OVERALL STANDARD DEVIATION OF THE DIFFERENTIAL PHASE SIGNAL (STDVDP, AVERAGE AND STANDARD DEVIATION) COMPARED WITH AVERAGE POROSITY FROM MATRIX DIGESTION FOR ALL NINE PLATES.

A higher correlation is observed when the two signals are averaged across the whole plates, however the mismatch between the STDVDP and the mid and lower porosity plates (below 4% porosity) is still visible. This again could be due to the fact that the resolution of the EI XPCi system is higher than the ultrasonic imaging system. However, the ultrasonic signal shows a variation in attenuation for plates below 2% porosity, whereas the STDVDP evaluation does not. This might be due to some of the features being below the system resolution for this low level of porosity, and as a result would have been detected by the dark field signal, hence the lack of variation in the STDVDP. The STDVDP needs to be investigated further, and its

relation to the dark field signal needs to be characterized in order to obtain a full understanding of porosity quantification in composite plates.

In order to correct for that, the STDVDP was compared to a destructive analysis method used for porosity estimation, matrix digestion, which was performed on samples taken from the same panels as the nine plates, from areas adjacent to where the plates were extracted. The porosity calculated for those plates using matrix digestion is compared to the STDVDP for all nine plates and shown in Fig. 7. The correlation observed between the porosity calculated from the matrix digestion and STDVDP for the nine plates is better than compared to the ultrasonic signal attenuation, with an R^2 of 0.99. Here, the correlation between the two signal is better for the mid- and low porosity plates (below 4%). However, for the low porosity plates (below 2%), the correlation is not as strong as for the rest of the plates. As mentioned above, this could be due to the fact that at those porosity values, some of the pores are small enough to show up within the dark field resolution as opposed to the STDVDP, meaning that the STDVDP only detects part of the porosity in those plates.

4. CONCLUSIONS

In this investigation, the porosity in carbon fiber reinforced woven composite plates was quantified using ultrasonic signal attenuation, matrix digestion, and planar EI XPCi, by introducing a new metric based on the standard deviation of the differential phase. This STDVDP metric, similar to the dark field signal, is capable of measuring variation in the distribution of the sample inhomogeneities, however for features of a scale equal to or above the system resolution (i.e., 12µm for the employed system). This new metric was proven to be capable of quantifying the porosity in composite plates as it showed a high correlation with both ultrasonic attenuation and matrix digestion. The comparison between the STDVDP and ultrasonic attenuation was done both on an ROI basis, as well as for the whole specimens. The comparison of the new metric with ultrasonic attenuation showed very good correlation both for the ROI and whole plate comparison. The ROI analysis showed good correlation for porosity variation within the specimens, however for plates with porosity below 4%, the correlation was not as strong. This is thought to be due to the size of some of the pores being below the system resolution, and as a result being detected by the dark field signal rather than the STDVDP.

When comparing the new STDVDP metric to porosity calculated from matrix digestion, an improved correlation was found, and the plates with porosity below 4% correlated better than with the ultrasonic signal attenuation. However, again for plates with porosity below 2%, the correlation did not hold as well. A possible explanation could be that the porosity size distribution in those plates spreads both below and above the resolution of the employed EI XPCi system (i.e., 12µm), meaning that some of the porosity is being detected using the STDVDP, whereas the smaller pores would be detected by the dark field signal.

The new approach using planar XPCi imaging shows great promise for the quantification of porosity in different types of composites in the future, especially its efficacy in doing so using only planar images, which cannot be done using other X-ray imaging methods. However, the nature of the new STDVDP metric and its relation to both the differential phase and the dark field signal need to be further investigated for varying pore size and shape distributions. Furthermore, this method should be applied to other types of composites, with different manufacturing methods, to ensure its efficacy.

ACKNOWLEDGEMENTS

This work was supported by the UK *Engineering and Physical Sciences Research Council* (*EPSRC*) [grant numbers EP/N509577/1 and EP/T005408/1]. A. Olivo is supported by the Royal Academy of Engineering under their Chairs in Emerging Technologies scheme.

REFERENCES

[1] L. Farhang and G. Fernlund, "Void and porosity characterization of uncured and partially cured prepregs," *J. Compos. Mater.*, vol. 50, no. 7, pp. 937–948, 2016.

[2] E. A. Birt and R. A. Smith, "A review of NDE methods for porosity measurement in fibre-reinforced polymer composites," *Insight Non-Destructive Test. Cond. Monit.*, vol. 46, no. 11, pp. 681–686, 2004.

[3] H. Jeong, "Effects of Voids on the Mechanical Strength and Ultrasonic Attenuation of Laminated Composites," *J. Compos. Mater.*, vol. 31, no. 3, pp. 276–292, 1997.

[4] P. Yang and R. Elhajjar, "Porosity Content Evaluation in Carbon-Fiber/Epoxy Composites Using X-ray Computed Tomography," *Polym. - Plast. Technol. Eng.*, vol. 53, no. 3, pp. 217–222, 2014.

[5] A. H. Kite, D. K. Hsu, and D. J. Barnard, "Determination of porosity content in composites by micrograph image processing," *AIP Conf. Proc.*, vol. 975, pp. 942–949, 2008.

[6] M. H. Hassan, A. R. Othman, and S. Kamaruddin, "Void content determination of fiber reinforced polymers by acid digestion method," *Adv. Mater. Res.*, vol. 795, 2013.

[7] A. Olivo and E. Castelli, "X-ray phase contrast imaging: From synchrotrons to conventional sources," *Riv. del Nuovo Cim.*, vol. 37, no. 9, pp.

467–508, 2014.
[8] V. Revol, B. Plank, R. Kaufmann, J. Kastner, C. Kottler, and A. Neels, “Laminate fibre structure characterisation of carbon fibre-reinforced polymers by X-ray scatter dark field imaging with a grating interferometer,” *NDT&E Int.*, vol. 58, pp. 64–71, 2013.
[9] S. C. Mayo, A. W. Stevenson, and S. W. Wilkins, “In-Line Phase-Contrast X-ray Imaging and Tomography for Materials Science,” *Materials*, vol. 5, no. 12, pp. 937–965, 2012.
[10] M. Endrizzi *et al.*, “Hard X-ray dark-field imaging with incoherent sample illumination,” *Appl. Phys. Lett.*, vol. 104, no. 2, pp. 3–6, 2014.
[11] C. Gusenbauer, M. Reiter, B. Plank, D. Salaberger, S. Senck, and J. Kastner, “Porosity Determination of Carbon and Glass Fibre Reinforced Polymers Using Phase-Contrast Imaging,” *J. Nondestruct. Eval.*, vol. 38, no. 1, pp. 1–10, 2019.
[12] F. Cosmi, A. Bernasconi, and N. Sodini, “Phase contrast micro-tomography and morphological analysis of a short carbon fibre reinforced polyamide,” *Compos. Sci. Technol.*, vol. 71, no. 1, pp. 23–30, 2011.
13] M. Endrizzi, B. I. S. Murat, P. Fromme, and A. Olivo, “Edge-illumination X-ray dark-field imaging for visualising defects in composite structures,” *Compos. Struct.*, vol. 134, pp. 895–899, 2015.
[14] D. Shoukroun *et al.*, “Enhanced composite plate impact damage detection and characterisation using X-Ray refraction and scattering contrast combined with ultrasonic imaging,” *Compos. Part B Eng.*, vol. 181, no. 107579, 2020.
[15] D. Shoukroun, L. Massimi, M. Endrizzi, D. Bate, P. Fromme, and A. Olivo, “Composite Porosity Characterization using X-ray Edge Illumination Phase Contrast and Ultrasonic Techniques,” in *Proceedings Volume 11593, Health Monitoring of Structural and Biological Systems XV*, 2021, p. 115932.
[16] L. Massimi *et al.*, “Detection of involved margins in breast specimens with X □ ray phase □ contrast computed tomography,” *Sci. Rep.*, vol. 11, no. 3663, pp. 1–9, 2021.
[17] M. Endrizzi, C. J. Maughan Jones, P. R. T. Munro, A. Olivo, and F. A. Vittoria, “Retrieval of weak x-ray scattering using edge illumination,” *Opt. Lett.*, vol. 43, no. 16, p. 3874, 2018.